Advanced Ceramics Progress: Vol. 12, No. 1, (Winter 2026) 36-45

Materials and Energy Research Center
MERC

Contents lists available at ACERP

Advanced Ceramics Progress

Journal Homepage: www.acerp.ir

Original Research Article

Experimental Investigation of the Effect of Tool Rotational Speed and Initial Workpiece Temperature in Dry Milling on Energy Consumption, Hardness Variation, and Corrosion Rate of AA6061 Aluminum Alloy

S.H. Pourhoseini [a], M.J. Tymouri [b], Sayyed Mohammadreza Sedehi [c,d] *, Mojtaba Vakili-Azghandi [e], M. Baghban [f]

[a] Associate Professor, Department of Mechanical Engineering, Faculty of Engineering, University of Gonabad, Gonabad, Iran.
[b] BSc Student, Department of Mechanical Engineering, Faculty of Engineering, University of Gonabad, Gonabad, Iran.
[c] PhD Student, School of Mechanical Engineering, College of Engineering, University of Tehran, Tehran, Iran.
[d] Chief Executive Officer (CEO), Farham Rad Mehr Co., Gonabad, Iran.
[e] Assistant Professor, Department of Materials Engineering, Faculty of Engineering, University of Gonabad, Gonabad, Iran.
[f] Assistant Professor, Department of Mechanical Engineering, Faculty of Engineering, University of Gonabad, Gonabad, Iran.

* Corresponding Author Email: mrsedehi@ut.ac.ir (S. M. Sedehi) URL: https://www.acerp.ir/article_252958.html

ARTICLE INFO

Article History:

Received 17 May 2026
Revised 22 July 2026
Accepted 03 September 2026

Keywords:

Milling,
Aluminum,
Corrosion,
Hardness,
Temperature,
Tool Rotational Speed

ABSTRACT

This study experimentally investigated the effects of tool rotational speed and initial workpiece temperature on energy consumption, surface hardness, and corrosion behavior of AA6061 aluminum alloy during milling. The results showed that energy consumption exhibited a nonlinear trend, initially decreasing and then increasing with increasing tool rotational speed and initial workpiece temperature, with minimum and maximum values of approximately 100–120 J and 170–190 J, respectively. Increasing energy input generally enhanced surface hardness up to an optimum level, whereas severe thermomechanical loading caused a slight reduction in hardness. XRD analysis also revealed a reduction in crystallite size and an increase in lattice strain under higher energy conditions. Overall, the controlled adjustment of machining parameters and energy consumption can effectively optimize surface hardness and microstructural evolution in AA6061.

https://doi.org/10.30501/acp.2026.582016.1196

1. INTRODUCTION

Milling is one of the key processes in metal machining, playing a decisive role in achieving dimensional accuracy, surface quality, and desirable mechanical properties (Zhenjing et al., 2025; Ullah et al., 2025). Owing to its high flexibility, capability for automated operation, and applicability to complex geometries, milling has been recognized as one of the fundamental manufacturing methods in modern industries, including automotive, aerospace, medical equipment, and tool manufacturing (Kundiya et al.,

Please cite this article as: Pourhoseini, S.H., Tymouri, M.J., Sedehi, S. M., Vakili-Azghandi, M., & Baghban, M. (2026). Experimental Investigation of the Effect of Tool Rotational Speed and Initial Workpiece Temperature in Dry Milling on Energy Consumption, Hardness Variation, and Corrosion Rate of AA6061 Aluminum Alloy. *Advanced Ceramics Progress*, *12*(1), 36-45. https://doi.org/10.30501/acp.2026.582016.1196

2025). Among engineering metals, aluminum occupies a prominent position due to its low density, high thermal conductivity, corrosion resistance, and excellent machinability (Mishra et al., 2025; Nyabadza et al., 2025). However, the unique thermal behavior of aluminum, along with its tendency for adhesion in the tool–workpiece contact zone, has made precise control of its machining conditions highly critical (Yadegari et al., 2025; Rathod & Wankhade, 2025; Zakaria et al., 2025). In the milling of aluminum, the quality of the final product is not only dependent on the intrinsic properties of the material but is also strongly influenced by process parameters such as cutting speed and the initial thermal condition of the workpiece (Nguyen & Le, 2025; Zhang et al., 2025). These factors simultaneously affect the material removal rate, heat distribution within the contact zone, frictional behavior at the tool interface, and ultimately the surface hardness and metallurgical structure of the machined component (Alsoufi & Bawazeer, 2025; Bai et al., 2025). In fact, milling can be considered a multivariable thermomechanical system in which thermal, mechanical, and kinematic effects interact with each other in a nonlinear manner (Michelacci et al., 2025).

Tool rotational speed is a critical parameter that directly influences cutting forces, strain rate, chip morphology, and surface roughness (Yang et al., 2025; Shanu et al., 2025). Excessive increases in rotational speed may lead to process instability and premature tool wear, whereas excessively low speeds reduce productivity and increase machining costs (Zhao et al., 2025). On the other hand, tool rotational speed, or cutting speed, governs the rate of heat transfer within the tool–workpiece interface and, if improperly adjusted, may result in excessive temperature rise, localized material softening, and deterioration of surface hardness (Guarise et al., 2025). Therefore, identifying an optimal balance among machining parameters remains a significant challenge from both industrial and academic perspectives. In most previous studies, it has been assumed that the initial temperature of the workpiece at the beginning of the milling process is equal to ambient temperature (Suresh Kumar et al., 2025; Bouhali et al., 2025). However, under actual manufacturing conditions, workpieces may be exposed to cold environments or pre-cooling processes prior to machining. Under such circumstances, an initial temperature lower than ambient temperature, for example, within the range of −3°C to room temperature, may significantly alter the thermal properties, coefficient of thermal expansion, and thermal conductivity of aluminum (Ali et al., 2025). A reduction in the initial temperature leads to a localized increase in yield strength, reduced ductility, and modifications in the chip formation mechanism (Damir et al., 2025). On the other hand, lower temperatures may reduce tool wear severity, as friction at the contact interface decreases and the stability of the cutting edge improves (Jaffery & Khan, 2025). These dual effects highlight the scientific importance of establishing an accurate relationship between initial temperature and final surface quality.

Over the past two decades, numerous researchers have focused on optimizing the milling conditions of aluminum alloys. For instance, several studies have employed the Taguchi method and analysis of variance (ANOVA) to determine the optimal levels of cutting speed and feed rate for minimizing surface roughness (Ayyıldız, 2025). Other researchers have utilized artificial neural networks and genetic algorithms to predict thermal behavior and cutting forces during the milling process (Hadjira et al., 2025). In addition, numerical simulations based on the finite element method have been developed to investigate stress and temperature distributions within the tool–workpiece interaction zone (Liu et al., 2025; Qian et al., 2025). Despite these advancements, limited studies have comprehensively examined the simultaneous effects of feed rate, tool rotational speed, and initial temperature on the mechanical behavior and final hardness of aluminum.

From a metallurgical perspective, the temperature distribution along the milling path, from tool entry to tool exit, may cause hardness heterogeneity across different regions of the machined component (Li & Li, 2005; Shen et al., 2021). Investigating hardness variations along the tool path can provide valuable insights into process stability, stress distribution, and microstructural evolution. In industrial environments, maintaining a stable initial workpiece temperature and accurately monitoring cutting speeds are among the major challenges. Factors such as environmental fluctuations, variations in cooling system performance, and tool wear can lead to unpredictable changes in machining outcomes (Niaki & Mears, 2017). Moreover, the interdependence among process parameters is such that a variation in one parameter may either amplify or mitigate the effect of another. This is particularly important in industries such as aerospace and automotive, where lightweight components with strict thermal tolerances are required (Sun et al., 2010). On the other hand, investigating sub-zero initial temperatures facilitates a deeper understanding of machining under cold conditions or in thermally controlled environments and may provide a foundation for the development of advanced cold machining technologies on an industrial scale. The novelty of the present study lies in investigating the combined effects of tool rotational speed and initial workpiece temperature, as well as analyzing their influence on process energy consumption and the evolution of surface hardness along the entire tool path, from tool entry to exit.

2. Materials and Methods

2.1. Raw Materials and Equipment

In this study, high-purity Aluminum Alloy 6061 was used as the base material. The precise chemical composition of this alloy, determined by SpectroMaxx Optical Emission Spectrometer (OES) analysis, is presented in Table 1.

material	Impurity content (mass%)
Al	96.85
Mg	0.9
Si	0.7
Fe	0.6
Cu	0.3
Cr	0.25
Zn	0.2
Ti	0.1
Others	0.1
Density (g/cm^3)	2/7
Particle size (um)	45

Table 1. Specifications of the Aluminum Used

Prior to the machining process, the specimens were cut into uniform dimensions of 100 × 50 × 10 mm using a wire-cutting process and subsequently polished with 1200-grit abrasive paper in order to eliminate initial surface effects. The milling experiments were performed using a three-axis CNC milling machine. A schematic illustration of the process setup and the experimental equipment is presented in Fig. 1. The cutting tool employed in this study was a tungsten carbide end mill coated with titanium aluminum nitride, featuring three active cutting edges, a positive rake angle, and a diameter of 10 mm. During the experiments, three primary process variables were investigated, including feed rate, tool rotational speed, and initial workpiece temperature. The initial temperature of the workpiece was controlled within a range from −2 °C to ambient temperature. To achieve sub-zero temperature conditions, a dry cooling chamber was employed in combination with a Type-K thermocouple sensor, with a measurement accuracy of ±0.1 °C. Table 2 shows the processing conditions of the specimens.

Figure 1. (a) Performing the Milling Process and (b) Real-Time Temperature Monitoring

Table 2. Nomenclature and Processing Conditions of the Specimens

Sample	Initial temperature	Tool rotation speed
0	Non Machined	
1	-2	1000
2	-2	1750
3	-2	2500
4	42	1000
5	42	1750
6	42	2500

3. Experimental Procedure and Characterization

During the experimental investigations, all parameters other than the selected variables were maintained constant in order to ensure an accurate comparison of the independent effect of each factor. To further investigate the phases present in the machined samples, XRD analysis was performed using an Explorer XRD manufactured by GNR Analytical Instruments Group under operating conditions of 40 kV and 30 mA. At the end of each machining path, the specimens were sectioned from the tool–workpiece contact region to the cutting exit zone, and localized surface hardness measurements were carried out along the feed direction. The hardness of the samples was measured using the Vickers hardness method with an INNOVATEST NEXUS 8000XL hardness tester, applying a load of 9.612 N and a dwell time of 15 s, in accordance with ASTM A370. To obtain reliable average values, each hardness test was repeated at least three times for every sample. In addition, corrosion behavior was evaluated in a simulated electrolyte environment using the potentiodynamic polarization technique. The electrochemical data, including corrosion potential, corrosion current density, and corrosion rate, were subsequently extracted and analyzed.

4. Results and Discussion

Fig. 2 shows the XRD results and magnified view of the main peak for the different machined aluminum samples. Based on the XRD patterns of the different machined aluminum samples, significant changes were observed in the position, intensity, and broadening of the diffraction peaks. In the reference sample (pure aluminum), the characteristic diffraction peaks were detected at 2θ values of approximately 38.4°, 44.6°, and 65.1°, corresponding to the (111), (200), and (220) crystallographic planes of the FCC aluminum structure, respectively (Sedehi et al., 2024). In the samples subjected to different milling conditions, an increase in tool rotational speed resulted in peak broadening, indicating changes in the surface crystallographic structure and a reduction in structurally disordered regions (Sedehi et al., 2025). On the other hand, the broadening of diffraction peaks may also indicate an increase in lattice strain and a reduction in effective grain size caused by the combined thermal and mechanical effects within the machined zone (Sedehi et al., 2022). The influence of the initial workpiece temperature was also clearly evident in the XRD patterns and was manifested through peak shifts relative to the reference sample, a phenomenon that has been attributed to lattice distortion in previous studies (Sedehi et al., 2022). Furthermore, in some samples machined under high rotational speeds, new diffraction peaks appeared within the range of 50° to 52°, which may be associated with the formation of aluminum oxide or intermetallic phases, or with surface phase transformations induced by localized high temperatures (Lisboa et al., 2014). These observations demonstrate the high sensitivity of the crystalline structure of aluminum to the combined thermal and mechanical conditions of the milling process. Overall, the XRD results confirmed that temperature and tool rotational speed exert a synergistic effect on surface microstructural evolution.

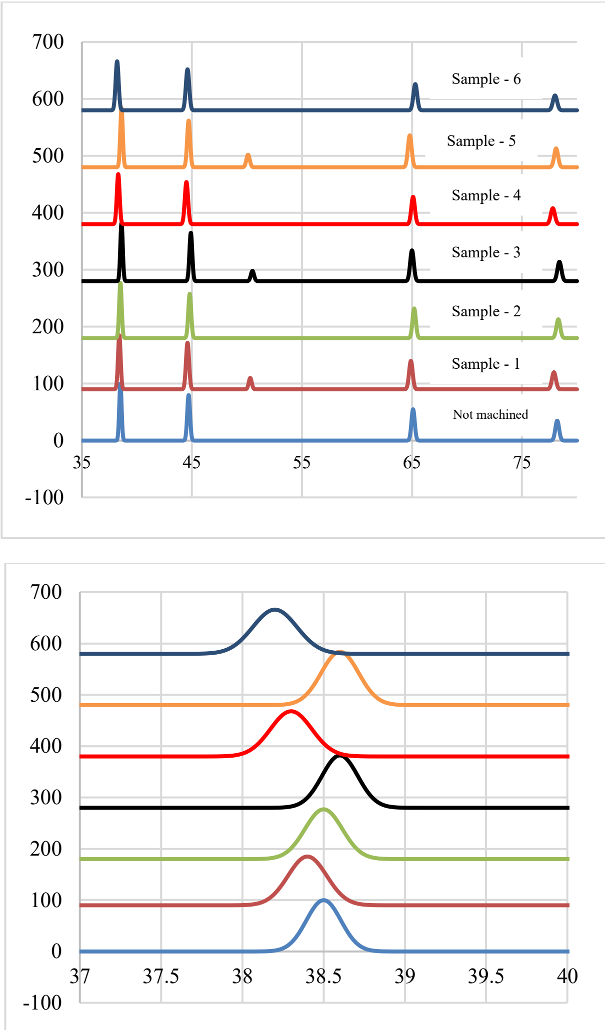

Figure 2. XRD Results and Magnified View of the Main Peak

The observation of the effects of cutting parameters on grain size is of particular importance, as grain refinement is considered a critical indicator for understanding process mechanics, especially the evolution of shear strain (Fergani & Liang, 2015). With increasing tool speed, the combined effects of elevated cutting temperature and strain rate significantly influence dynamic recrystallization; however, beyond a critical threshold, excessive thermal input may substantially suppress grain refinement (Fergani & Liang, 2015). Excessive rotational speed increases localized temperature and facilitates recrystallization, whereas the increase in thermal energy also intensifies lattice strain and contributes to grain size reduction (Fergani & Liang, 2015). Conversely, reducing the initial workpiece temperature limits atomic mobility, leading to the formation of defect-rich microstructures (Nwaokafor et al., 2021).

Therefore, it can be concluded that an optimal combination of these two parameters can establish a desirable balance among crystallographic density, grain size, and residual lattice strain. These findings provide a fundamental basis for interpreting hardness measurements and correlating crystallographic evolution with the mechanical behavior of the machined samples in the subsequent stages of this researc (Kumar et al., 2016).

4.1. Variation of Hardness with Temperature, Tool Rotational Speed and Along the Tool Path

Fig. 3 shows the hardness variations in terms of tool rotational speed and initial temperatures and Table 3 shows hardness variations along the processing path. The analysis of hardness variations with respect to tool rotational speed and initial temperature indicates that the starting temperature of the process can fundamentally alter the influence of rotational speed. At low initial temperatures, increasing the tool rotational speed leads to pronounced fluctuations in hardness along the tool path, reflecting a high sensitivity of the material to abrupt thermal changes (Samples 1 to 3). Under these conditions, any increase in rotational speed significantly elevates the heat generation rate, resulting in microstructural inhomogeneity due to non-uniform thermal exposure and localized deformation. In contrast, at elevated initial temperatures, the effect of increasing tool rotational speed on hardness variation becomes noticeably more moderate (Samples 4 to 6). In this regime, the material is already in a thermally activated state in which recovery and dislocation rearrangement are facilitated; therefore, the additional thermal input induced by higher rotational speeds does not lead to severe hardness fluctuations. Furthermore, the results indicate that at higher temperatures, even at elevated rotational speeds, the reduction in hardness toward the end of the tool path is less pronounced. This behavior can be attributed to a reduced thermal gradient and a more homogeneous distribution of thermally induced stresses. The convergence of these observations suggests that selecting tool rotational speed without considering the initial temperature can lead to inaccurate predictions of surface mechanical behavior, as thermomechanical coupling plays a dominant role in governing hardness evolution.

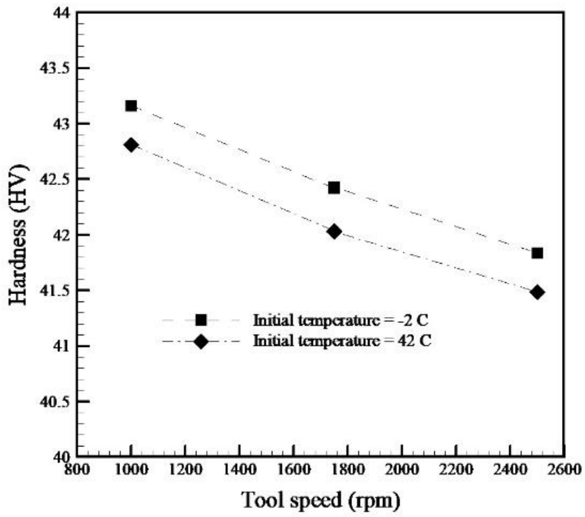

Figure 3. Hardness Variations as a Function of Tool Rotational Speed and Temperature Changes

4.2. Corrosion Variation Along the Tool Path as a Function of Temperature and Tool Rotational Speed

Table 3. Hardness Variations Along the Processing Path

Sample	entry point				exit point
1	42/5	42.5	42.2	41.8	42.3
2	42/9	41.4	40.9	41.0	41.7
3	42/6	42.1	42.6	41.3	41.7
4	40.8	40.6	40.3	40.0	40.4
5	41.1	39.8	39.4	39.6	40.1
6	40.7	40.2	40.6	39.5	39.9

The corrosion variation results as a function of temperature and tool rotational speed are shown in Fig. 4 and summarized in Table 4. The Tafel polarization profiles indicate that the specimens under three optimized machining conditions (based on the hardness results) exhibit significantly different corrosion behaviors. Specifically, the corrosion potentials were measured as −0.421 V for Sample 1, −0.578 V for Sample 2, and −0.599 V for Sample 3, indicating noticeable differences in the electrochemical stability of the surface layer. The anodic slope of Sample 2 was approximately 0.0940, while its cathodic slope was 0.0698, suggesting more stable oxidation and reduction reactions and the formation of a more uniform passive layer. This behavior is consistent with previous reports, which attribute such improvements to grain refinement and a more homogeneous distribution of surface stresses, facilitating the formation of a more stable oxide layer (Wei et al., 2025).

The calculated corrosion rates based on the corrosion current density (i_{corr}) also show significant differences among the samples. Sample 3 exhibited the best corrosion resistance, with a rate of 0.0079 mm/year, while Sample 2 and Sample 1 showed higher rates of 0.024 mm/year and 0.031 mm/year, respectively. The higher corrosion rate of Sample 1 can be attributed to the presence of micro-discontinuities and surface heterogeneities, which enhance chloride ion penetration. In Sample 2, machining-induced heat likely promoted the formation of relatively weak and less stable oxide layers, which may act as initiation sites for localized and pitting corrosion (Zhang et al., 2026).

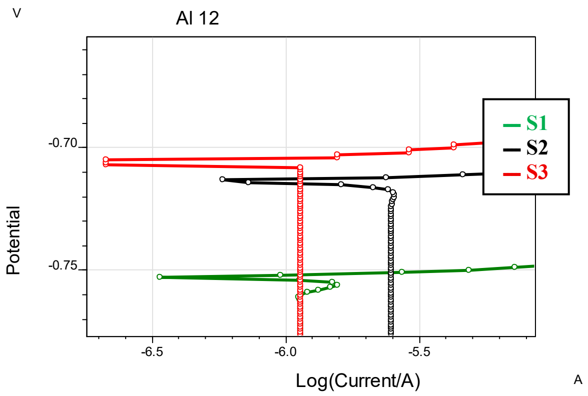

Figure 4. Corrosion Results as a Function of Tool Rotational Speed and Temperature Variations

Table 5. Values of the Corrosion Test Results

Parameter	S1	S2	S3
E_{corr} (V vs. Ag/AgCl)	-0.421	-0.578	-0.599
i_{corr} (A)	2.9615×10^{-6}	1.4532×10^{-6}	1.0441×10^{-6}
b_a (V/decade)	0.0938	0.0940	0.06845
b_c (V/decade)	0.10635	0/0698	0.09458
R_p (ohm)	8311.9	12975	16518
Corrosion rate (mm/year)	0.031	0.024	0.0079

A comparison of anodic and cathodic behavior further reveals that Sample 3, with a higher polarization resistance (Rp ≈ 15974 Ω), exhibits superior electrochemical stability, as evidenced by a slower increase in current density in the anodic region, indicating a more stable passive film and a reduced tendency for selective dissolution. Additionally, the higher hardness and the presence of compressive residual stresses in this sample reduce the number of active anodic sites, thereby shifting the corrosion mechanism from an aggressive localized mode to a more controlled uniform mode. Previous studies have also confirmed that compressive stresses and refined grain structures reduce passive film breakdown and slow its growth and rupture processes, ultimately enhancing corrosion resistance (Yelwa et al., 2025).

4.3. Potentiodynamic Polarization Curves under Linear Sweep Voltammetry (LSV)

The potentiodynamic polarization curves shown in Fig. 5 illustrate the electrochemical behavior of the samples in a NaCl environment. In chloride-containing media, Cl^- ions directly attack the naturally formed aluminum oxide layer, leading to localized defects in the Al_2O_3 passive film.

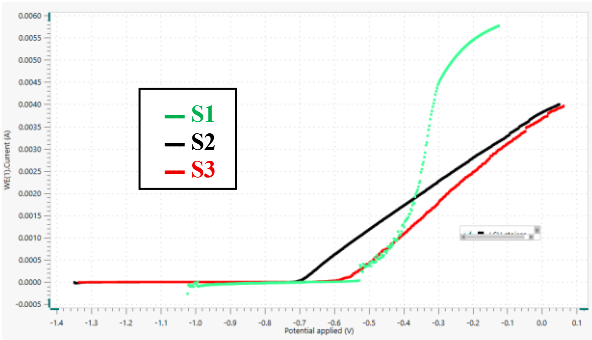

Figure 5. Linear Sweep Voltammetry (LSV) Polarization Curves of the First to Third Specimens

From the current–potential plots, it can be observed that Sample 2 departs from the near-zero current regime earlier than the other two samples, indicating faster chloride ion penetration and an earlier onset of localized dissolution. This behavior is typically associated with a higher density of defects, increased porosity, or reduced passive film thickness. Sample 3 maintains a low current response over a wider potential range, and its current increases more gradually, indicating greater stability of the passive film against chloride adsorption and a delayed initiation of pitting corrosion. In contrast, although Sample 1 shows relatively stable behavior up to approximately −0.45 V, once the critical potential is reached, it exhibits a very sharp increase in current density. This reflects sudden passive film breakdown and rapid pit propagation, which in NaCl environments is commonly attributed to localized chloride accumulation at surface weak points and the acceleration of the anodic reaction $Al \rightarrow Al^{3+}$.

From an engineering perspective in NaCl solutions, the key controlling parameters are the breakdown potential and the magnitude of the current density after breakdown. Sample 2 activates earlier due to its lower breakdown potential, making it more susceptible to pitting corrosion. Sample 1, although exhibiting a higher breakdown potential, undergoes severe dissolution once degradation begins, potentially leading to deep and hazardous pit formation, which is critical for components exposed to high electrochemical stress. Sample 3 demonstrates more balanced behavior, neither activating prematurely nor showing an abrupt current surge, indicating a more stable passive film and a more uniform distribution of electrochemical stresses in the presence of chloride ions. Therefore, in terms of overall resistance to pitting corrosion and controlled degradation in NaCl environments, Sample 3 exhibits superior engineering performance. Fig. 6 shows the SEM images of the three optimized specimens in terms of hardness and corrosion properties. To further investigate the microstructure developed during the machining process, SEM images were obtained for the first three specimens. The presence and distribution of the observed pores provide a basis for correlating the SEM observations with the corrosion results, as these pores can facilitate localized corrosion and consequently reduce the corrosion resistance of the specimens.

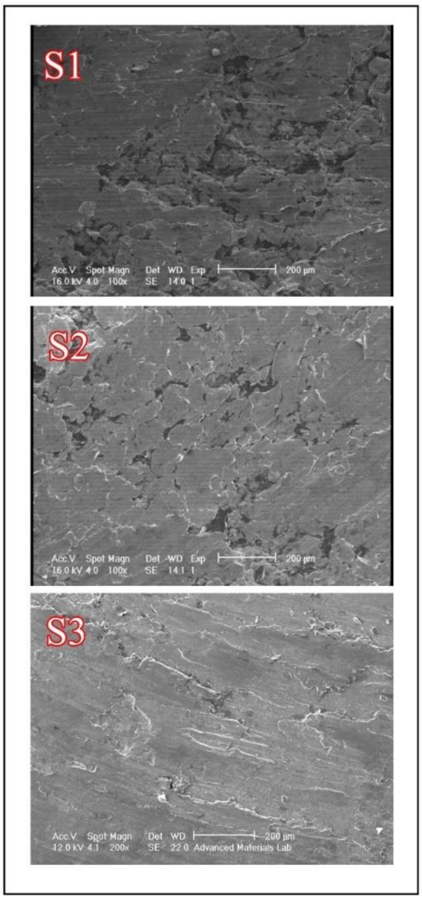

Figure 6. SEM Images of the Three Optimized Specimens in Terms of Hardness and Corrosion Properties

4.4. Effect of Initial Temperature and Tool Rotational Speed on Energy Consumption

Machining processes, which are predominantly composed of machine tool operations, are widely used across various industrial applications and generally exhibit low energy efficiency. Consequently, they present significant potential for energy savings and the reduction of greenhouse gas emissions. To achieve such energy savings, accurate prediction of machining energy consumption is essential. Moreover, it can serve as a decision-support tool for defining energy quotas, optimizing cutting parameters for energy efficiency, and evaluating overall energy performance. Several relevant studies on machining energy prediction have been reported. Dietmair and Verl (Dietmair et al., 2009) proposed a modeling framework for predicting machine tool energy consumption and provided strategies for applying the model to energy optimization. Kara and Li (Kara et al., 2011) developed an empirical approach for constructing unit process energy consumption models for material removal processes, which was validated across eight different CNC turning and milling machines. Their model was able to predict machining energy consumption with an accuracy exceeding 90%.

The combined effect of initial temperature and tool rotational speed on energy consumption indicates that these two parameters are strongly coupled and significantly influence both power demand and process efficiency. Increasing rotational speed generally leads to higher instantaneous energy consumption; however, the initial temperature can either mitigate or amplify this effect. At low temperatures, a larger portion of energy is required to overcome plastic deformation resistance (Samples 1 to 3) (Lu et al., 2015). At higher initial temperatures, part of the required deformation energy is supplied by the stored thermal energy within the workpiece. As a result, even at higher rotational speeds, energy consumption does not increase linearly (Samples 3 and 6). At the same time, the more uniform hardness distribution along the machining path indicates that the input energy is being consumed more uniformly throughout the process. Finally, the overlap among hardness, corrosion, and energy analyses suggests that conditions leading to severe hardness fluctuations and hardness degradation at the exit region are generally associated with higher energy consumption and lower process efficiency. Therefore, simultaneous control of initial temperature and tool rotational speed is not only essential for improving mechanical properties but also crucial for optimizing energy consumption and enhancing overall machining efficiency.

4. Conclusion

In this study, the effects of two key parameters, initial workpiece temperature and tool rotational speed, on the microstructural evolution and surface hardness of aluminum were systematically investigated. The results clearly demonstrated that the hardness evolution along the dry-machining path of aluminum is strongly influenced by the combined effects of initial workpiece temperature and rotational speed. The effect of each parameter was found to depend on the level of the other, indicating that independent evaluation of these parameters cannot fully describe the mechanical response of the material. The data indicate that initial temperature plays a critical regulatory role, capable of either amplifying or mitigating the effects induced by increasing tool rotational speed.

Among the investigated interactions, the synergistic effect of temperature and cutting speed showed the most significant influence on hardness stability along the machining path. Higher initial temperatures, particularly when combined with elevated rotational speeds, resulted in a more uniform hardness distribution, reduced local fluctuations, and improved energy behavior of the process. This highlights the importance of controlled preheating or proper thermal conditioning prior to machining. It was also observed that excessive increases in tool rotational speed, regardless of other conditions, can lead to hardness degradation at the end of the cutting path and higher energy consumption. Therefore, process optimization should not be based solely on increasing kinematic parameters but rather on achieving a balance among strain rate, heat generation, and tool–workpiece interaction time. Overall, this study demonstrates that, through intelligent selection of process parameter combinations, it is possible to simultaneously reduce energy consumption and improve surface quality and hardness uniformity in the dry machining of aluminum. These findings can serve as practical guidelines for designing stable and cost-effective process windows in industries relying on coolant-free machining operations.

Acknowledgements

The authors gratefully acknowledge the support and assistance provided by the laboratory staff and affiliated research institutions during this study.

References

1. Ali, N. H. O., Admi, A. E., Osman, S. A., & Osman, S. A. (2025). Effect of coolant concentration ratio on surface roughness in machining aluminium 6061: A case study. *Journal of Advanced Research in Experimental Fluid Mechanics and Heat Transfer, 18*(1), 55–68. https://doi.org/10.37934/arefmht.18.1.5568

2. Alsoufi, M. S., & Bawazeer, S. A. (2025). Probabilistic analysis of surface integrity in CNC turning: Influence of thermal conductivity and hardness on roughness and waviness distributions. *Machines, 13*(5), 385. https://doi.org/10.3390/machines13050385

3. Ayyıldız, M. (2025). Optimization and prediction of surface roughness in the milling process of aluminum alloy using Taguchi method and artificial neural network. *Multidiscipline Modeling in Materials and Structures, 21*(5), 1204–1216. https://doi.org/10.1108/MMMS-02-2025-0059

4. Bai, T., Wang, X., Gao, Z., Wang, S., Zuo, C., Kang, J., ... & Zhang, J. (2025). Tool wear analysis of high-speed sawing of aerospace aluminum alloy based on FEM simulation and cutting experiments. *Journal of Manufacturing Processes, 139*, 193–209. https://doi.org/10.1016/j.jmapro.2025.02.033

5. Bouhali, R., Bendjeffal, H., Chetioui, K. B., & Bousba, I. (2025). Multivariable optimization based on the Taguchi method to study the cutting conditions in aluminum turning. *International Journal on Interactive Design and Manufacturing (IJIDeM), 19*(5), 3541–3551. https://doi.org/10.1007/s12008-024-01995-9

6. Damir, A., Shi, B., Elsayed, A., Thelin, J., M'Saoubi, R., & Attia, H. (2025). On the tribological and thermal aspects of cryogenic machining of Inconel 718 and their effects on surface integrity. *Wear, 571*, 205855. https://doi.org/10.1016/j.wear.2025.205855

7. Dietmair, A., & Verl, A. (2009). Energy consumption forecasting and optimisation for tool machines. MM Science Journal, March 2009. https://doi.org/10.17973/MMSJ.2009_03_20090305

8. Fergani, O., & Liang, S. Y. (2015). The effect of machining process thermo-mechanical loading on workpiece average grain size. The International Journal of Advanced Manufacturing Technology, 80(1–4), 21–29. https://doi.org/10.1007/s00170-015-6975-8

9. Guarise, A., Bertolini, R., Ghiotti, A., & Bruschi, S. (2025). Wear behaviour of additively manufactured Nitinol cryogenically machined at different cutting speeds. *Tribology International, 204*, 110478. https://doi.org/10.1016/j.triboint.2024.110478

10. Hadjira, L., Nesrine, M., Oussama, B., Mustapha, T., Yapan, Y. F., & Uysal, A. (2025). Evaluation of nano-MoS_2-assisted MQL performances in end milling of AISI 316L austenitic stainless steel and multi-objective optimization via genetic algorithm. *The International Journal of Advanced Manufacturing Technology, 141*(3–4), 1469–1484. https://doi.org/10.1007/s00170-025-16763-6

11. Jaffery, S. H. I., & Khan, M. A. (2025). Tool wear analysis of turning Ti-6Al-4V under dry, wet and cryogenic conditions. *Procedia CIRP, 135*, 533–537. https://doi.org/10.1016/j.procir.2024.12.055

12. Kara, S., & Li, W. (2011). Unit process energy consumption models for material removal processes. CIRP Annals, 60(1), 37–40. https://doi.org/10.1016/j.cirp.2011.03.018

13. Kumar, S., Mote, V. D., Prakash, R., & Kumar, V. (2016). X-ray analysis of α-Al_2O_3 particles by Williamson–Hall methods. Materials Focus, 5(6), 545–549. https://doi.org/10.1166/mat.2016.1345

14. Kundiya, R. R., Kadam, M., Jadhav, P., & Pawade, R. (2025). A review on high speed micro-milling of shape memory alloy (NiTinol): Process and post perspective. *International Journal on Interactive Design and Manufacturing (IJIDeM), 19*(4), 2337–2353. https://doi.org/10.1007/s12008-024-02153-x

15. Li, J., & Li, J. C. M. (2005). Temperature distribution in workpiece during scratching and grinding. *Materials Science*

and Engineering: A, 409(1–2), 108–119. https://doi.org/10.1016/j.msea.2005.07.057

16. Lisboa, A. J. T., Vasconcelos, N. S. L. S., Rangel, J. H. G., Oliveira, M. M. O., Longo, E., Varela, J. A., & Vasconcelos, J. S. (2014). Study of the thermal resistance of alpha-phase aluminum oxide (α-Al_2O_3) films deposited on the paper substrate. Ceramics International, 40(7), 9509–9516. https://doi.org/10.1016/j.ceramint.2014.02.024

17. Liu, H., Meurer, M., & Bergs, T. (2025). Experimental and Finite Element Analysis of adapted cutting fluid supply on tool temperature and wear progression in Inconel 718 turning. *Journal of Manufacturing Processes, 137*, 166–180. https://doi.org/10.1016/j.jmapro.2025.01.061

18. Lu, X., Jia, Z., Wang, X., Li, G., & Ren, Z. (2015). Three-dimensional dynamic cutting forces prediction model during micro-milling nickel-based superalloy. The International Journal of Advanced Manufacturing Technology, 81(9–12), 2067–2086. https://doi.org/10.1007/s00170-015-7310-0

19. Michelacci, F. D., Han, G., & Kim, S. (2025). Autonomous process optimization of a tabletop CNC milling machine using computer vision and deep learning. *CIRP Journal of Manufacturing Science and Technology, 60*, 153–164. https://doi.org/10.1016/j.cirpj.2025.04.009

20. Mishra, T. N., Kumar, A., & Prasad, S. B. (2025). A recent innovation in stir-cast aluminium metal matrix composites to improve mechanical and wear properties with potential applications: A review. *JOM, 77*(10), 7895–7924. https://doi.org/10.1007/s11837-025-07570-1

21. Nguyen, V. H., & Le, T. T. (2025). Predicting surface roughness in machining aluminum alloys taking into account material properties. *International Journal of Computer Integrated Manufacturing, 38*(4), 555–576. https://doi.org/10.1080/0951192X.2024.2372252

22. Niaki, F. A., & Mears, L. (2017). A comprehensive study on the effects of tool wear on surface roughness, dimensional integrity and residual stress in turning IN718 hard-to-machine alloy. *Journal of Manufacturing Processes, 30*, 268–280. https://doi.org/10.1016/j.jmapro.2017.09.016

23. Nwaokafor, P., Okeoma, K. B., Echendu, O. K., Ohajianya, A. C., & Egbo, K. O. (2021). X-ray diffraction analysis of a class of AlMgCu alloy using Williamson–Hall and Scherrer methods. Metallography, Microstructure, and Analysis, 10(6), 727–735. https://doi.org/10.1007/s13632-021-00792-0

24. Nyabadza, A., McCarthy, É., Makhesana, M., Heidarinassab, S., Azoulay-Younes, L., O'Toole, K., ... & Brabazon, D. (2025). A review of carbon and aluminium nanofluids and elastocaloric materials for heating and cooling applications. *International Journal of Thermofluids, 27*, 101163. https://doi.org/10.1016/j.ijft.2025.101163

25. Qian, N., Sun, B., Li, M., Wang, J., Yang, L., Das, R., ... & Xu, J. (2025). Mechanism of cutting damage formation and turning process optimization of 3D needled C/SiC composites. *Journal of the European Ceramic Society, 45*(7), 117234. https://doi.org/10.1016/j.jeurceramsoc.2025.117234

26. Rathod, V. P., & Wankhade, S. H. (2025). A review on impact of micro-tools on micro-milling outcomes for aluminium alloy. *Advances in Science and Technology Research Journal, 19*(3), 322–340. https://doi.org/10.12913/22998624/200007

27. Sedehi, S. M. R., Khosravi, M., & Yaghoubi Nejad, Y. (2022). Experimental comparison of microstructure and surface properties of Al/Al_2O_3 sample produced by powder metallurgy and spark plasma sintering methods. Journal of Solid and Fluid Mechanics, 12(5), 123–132. 10.22044/jsfm.2022.11821.3580

28. Sedehi, S. M., Samarghandi, M., Samarghandi, A., & Maraki, M. (2024). The effect of simple shear extrusion on the microstructure and surface properties of aluminum components produced by powder metallurgy. Iranian Journal of Materials Forming, 11(1), 24–33. 10.22099/ijmf.2024.49501.1282

29. Sedehi, S. M. R., Norouzi Palangani, F., Maleki, Z., & Banihashemi, S. F. (2025). Effect of Conventional and Climb Milling on the Mechanical Properties and Biocompatibility of Pure Titanium; Application of the Williamson-Hall Method. Iranian Journal of War and Public Health, 17(1), 51–61. https://doi.org/10.58209/ijwph.17.1.51

30. Shanu, A., Singh, R., & Dixit, P. (2025). Synergistic roles of steady dwell tool feeding and ultrasonic vibrations in electrochemical discharge machining of alumina. *Materials and Manufacturing Processes, 40*(1), 20–36. https://doi.org/10.1080/10426914.2024.2406775

31. Shen, X., Zhang, D., & Tan, L. (2021). Effects of cutter path orientations on milling force, temperature, and surface integrity when ball end milling of TC17 alloy. *Proceedings of the Institution of Mechanical Engineers, Part B: Journal of Engineering Manufacture, 235*(6–7), 1212–1224. https://doi.org/10.1177/0954405420971070

32. Sun, S., Brandt, M., & Dargusch, M. S. (2010). Thermally enhanced machining of hard-to-machine materials—a review. International Journal of Machine Tools and Manufacture, 50(8), 663–680. https://doi.org/10.1016/j.ijmachtools.2010.04.008

33. Suresh Kumar, R., Naveen, S., Suresh, V., & Madhu, S. (2025). Novel approach to monitoring the surface integrity of aluminum 5052 using sound and vibration signals during turning with titanium-coated carbide inserts. *Journal of Materials Engineering and Performance, 34*(12), 11871–11880. https://doi.org/10.1007/s11665-024-09883-9

34. Ullah, N., Rehan, M., Farooq, M. U., Li, H., Yip, W. S., & To, S. S. (2025). A comprehensive review of micro-milling: fundamental mechanics, challenges, and future prospective. *The International Journal of Advanced Manufacturing Technology, 137*(9–10), 4309–4351. https://doi.org/10.1007/s00170-025-15388-z

35. Wei, Q., Wang, X., Lu, Y., Cheng, Z., Dong, H., Wang, X., ... & Shen, Q. (2025). Enhanced wear resistance of AISI 1045 steel by TiAlN/CrN gradient coatings via toughness-hardness synergy. Thin Solid Films, 826, 140756. https://doi.org/10.1016/j.tsf.2025.140756

36. Yadegari, M. J., Martucci, A., Biamino, S., Ugues, D., Montanaro, L., Fino, P., & Lombardi, M. (2025). Aluminum laser additive manufacturing: A review on challenges and opportunities through the lens of sustainability. *Applied Sciences, 15*(4), 2221. https://doi.org/10.3390/app15042221

37. Yang, H. D., Zhang, L. B., Li, H. D., Zhang, J. S., Tang, H. H., & Chen, S. H. (2025). Influence of tool corner radius on chip geometrical characteristics of machining Zr-based bulk metallic glass. *Journal of Advanced Manufacturing Science and Technology, 5*(2), 2025012. https://doi.org/10.51393/j.jamst.2025012

38. Yelwa, J. M., Musa, H., Fasanya, O. O., & Yahaya, J. Y. (2025). Corrosion-resistant coatings: advances in deposition methods, nanostructures, and self-healing films. Academia Materials Science, 2(3). https://doi.org/10.20935/AcadMatSci7829

39. Zakaria, H., Silai, Z., Hussain, G., Domblesky, J. P., Kong, J., Louhichi, B., & Wei, H. (2025). In-process and post-machining corrosion of aluminum alloys: Mechanisms, root causes, and inhibitive approaches. *Materials Today Chemistry, 48*, 102897. https://doi.org/10.1016/j.mtchem.2025.102897

40. Zhang, S., Li, L., Zhao, Z., Li, Y., Shen, L., & Zhang, S. (2025). Enhanced electron transfer for superior Cr(VI) removal in water using ball-milled aluminum/biochar composite with embedded structure: Efficiency and mechanism. *Separation and Purification Technology, 362*, 131809. https://doi.org/10.1016/j.seppur.2025.131809

41. Zhang, S., He, J., Wang, D., Wang, Y., & Duan, L. (2026). Dynamic corrosion mechanisms and electrochemical correction factors in solid waste incineration environments. Chemical Engineering Science, 319, 122231. https://doi.org/10.1016/j.ces.2025.122231

42. Zhao, Y., Zhang, J., Li, L., Goel, S., Zhang, C., Wu, X., ... & Guo, J. (2025). Evolution of tool wear and machining quality during dry milling of $AlCoCrFeNi_{2.1}$ eutectic high entropy alloy. *Wear, 560–561*, 205616. https://doi.org/10.1016/j.wear.2024.205616

43. Zhenjing, D. U. A. N., Ziheng, W. A. N. G., Shuaishuai, W. A. N. G., Peng, B. I. A. N., Yuheng, L. I., Jiyu, L. I. U., ... & Xin, L. I. U. (2025). Tool wear in enhanced minimum quantity lubrication assisted milling: from mechanism to application. Chinese Journal of Aeronautics, 103597. https://doi.org/10.1016/j.cja.2025.103597